9th AUSTRALASIAN
FLUID MECHANICS CONFERENCE,
AUCKLAND, 8-12 DECEMBER 1986

Wind Tunnel Contraction Design

JONATHAN H. WATMUFF

Gas Dynamics Laboratory, Department of Mechanical & Aerospace Engineering, Princeton University, Princeton, New Jersey 08544, U.S.A.

INTRODUCTION

Since the flow is accelerated by a wind tunnel contraction the pressure gradients on the walls are generated favorable. However, for finite length contractions two regions of adverse pressure gradient exist near the entry and exit. As a result the velocity profile across the exit plane of a contraction is non-uniform leading to a reduction of useful length of the working section. Furthermore, the two regions of adverse pressure may cause large-scale intermittent boundary layer separation resulting in increased unsteadiness of the flow in the working section. It is well known (e.g. Bradshaw 1973) that boundary layers are more unstable over concave surfaces (e.g. near a contraction inlet) than those over convex surfaces (e.g. near a contraction exit). Therefore a smaller adverse pressure gradient can be tolerated near the entry compared to the exit of a contraction to avoid boundary layer separation.

Most analytical methods of contraction design have been based on Stokes' Stream Function for the steady axisymmetric flow of an incompressible inviscid fluid i.e.

$$\frac{\partial^2\psi}{\partial x^2} - \frac{1}{r}\frac{\partial\psi}{\partial x} + \frac{\partial^2\psi}{\partial r^2} = 0 \qquad (1)$$

where x and r are coordinates in the axial and radial directions and U and V are the respective fluid velocities given by

$$U = \frac{1}{r}\frac{\partial\psi}{\partial r} \text{ and } V = -\frac{1}{r}\frac{\partial\psi}{\partial x}$$

Most analytical solutions have been found by the method of separation of variables of equation (1). Depending on the choice of separation constant, three possible series solutions may be constructed. Each of these types of solutions from serious shortcomings. The first type is restricted to families of axial velocity distributions which permit analytical expression of their derivatives e.g. Tsien (1943), Szceniowski (1943) and more recently Cohen and Ritchie (1962). The major difficulty in applying this type of solution arises from the stringent requirements on the form of the axial velocity distribution. Barger and Bowen (1972) generalized the method to cater for a wider range of velocity distributions so that the method could be applied to a greater variety of duct shapes. Nevertheless, this approach is still restrictive in the sense that only a limited number of contraction shapes can be obtained from the solutions. The second type of solution is periodic in the streamwise direction e.g. Thwaites (1946) obtained series solutions in terms of Bessel functions. Since equation (1) is elliptic the effect of periodic repetition of the contraction shape will give a flow different to that with upstream and downstream sections of constant area. The third type of solution is in the form of an aperiodic (exponential) series which produces solutions for the contraction shape which are infinitely long. A practical design based on this type of solution needs to be truncated, and the truncation may produce unknown and undesirable effects. Other techniques that have been tried include Smith and Wang (1944) who used a distribution of singularities such as ring vortices, sources and sinks to design a family of contractions. It is unfortunate that there has been little experimental confirmation of the adequacy of these analytical methods. Faced with these difficulties many designers have merely sketched plausible shapes by eye or selected a contour used elsewhere and believed to be acceptable.

Batchelor and Shaw (1944) were one of the first to apply numerical methods to examine the flow properties of an axisymmetric contraction and they performed the laborious computations for the current LSWT contraction by hand. The design is characterized by an initially rapid rate of contraction followed by a more gradual variation near the exit. The results of their computations led them to suspect that the inlet boundary layer of the LWST may suffer from intermittent boundary layer separation causing increased unsteadiness of the flow in the working section.

Morel (1975) carried out a study aimed at the providing practical guidelines for the design of axisymmetric contractions. Contours formed by two power law arcs joined smoothly together at an inflection point were examined. Cubic polynomials were found to form the most suitable wall shape and these were selected for a detailed study. Finite-difference solutions of the Euler equations were used to produce design charts which define the contraction length and position of the inflection point in terms of allowable adverse pressure gradients at the inlet and the exit and the desired exit flow uniformity. Morel was the first to show the remarkable fact that for fixed requirements, the contraction length decreases as the contraction ratio increases.

Mikhail (1979) proposed a method for the optimum design of a wind tunnel contraction defined to be the shortest one that avoids boundary layer separation and which supplies the flow to the working section with a specified uniformity. Boundary layer calculations were made using a computer program based on the "lag-entrainment" method which takes into account the wall curvature. He showed that by optimizing the contraction wall curvature it is possible to reduce the contraction length considerably. However the behaviour of turbulent boundary layers with extra strain rates (such as those caused by streamline curvature or pressure gradients) is still the subject of current research. It is doubtful whether separation can be accurately predicted on a contraction wall where the boundary layers experience both streamline curvature and pressure gradients.

NUMERICAL TECHNIQUES

A calculation method has been developed by the author for the solution of Stokes' Stream Function, i.e. equation (1). The code was written in FORTRAN 77 and was developed and run on a 16-bit PDP 11/23-PLUS microcomputer. Suitable boundary conditions for a contraction are:

(1) $\psi = 0$ along the axis.

(2) $\psi = \psi_w$ = constant, along the boundary.

(3) $\psi = \left(\frac{r}{r_w}\right)^2 \psi_w$ across the entry to the region of constant cross-sectional upstream of the contraction (r_w = radius of tunnel boundary). This gives $U = 2\,\psi_w/r_w^2$ = constant. If the length of the parallel-walled entry region is large then the radial velocity component will be small and the entry flow will be very nearly uniform and parallel to the axis.

(4) $\frac{\partial^2\psi}{\partial x^2} = 0$ across the exit of the region of constant cross-sectional area downstream of the contraction.

Integration of the governing differential equation with the prescribed boundary conditions is accomplished using the relaxation method. Details of the method can be found in undergraduate textbooks (e.g. Smith 1978). No attempt was made to use a non-uniform grid to cope with the larger gradients of the stream function experienced near the tunnel walls, nor was a coordinate transformation utilized to make the calculation domain rectangular (e.g. Mikhail 1979). The iterations were continued until all nodal values remained unchanged from their previous value i.e. the results had converged to around 7 significant figures. The total computational time varies approximately as N^3 (where N = number of axid grid lines = the number of radial grid lines). For the results presented here, N = 60, taking around 15 hours (i.e. an overnight run) and performing around 4000 iterations.

Since the governing equation is elliptic in the flow within the contraction is sensitive to the upstream and downstream flow conditions. Therefore it is important that the lengths of the constant area sections before and after the contraction are large enough to have negligible influence on the results. Morel (1975) used inlet and outlet extensions that were 0.7 local diameters in length. He reports that further lengthening had no influence on his results but made no mention of the effects of shortening the extensions. A series of calculations were made using equal inlet/outlet extensions of lengths 0.125, 0.225, 0.325 and 0.425 inlet diameters for the cubic contraction shape shown in Figure 6. The C_p contours revealed that only the contours near the inlet and outlet of the contraction with nondimensional inlet/outlet extension length of 0.125 were significantly effected i.e. differences between the contours for the other cases were undetectable. Therefore inlet/outlet extensions that are 0.225 inlet diameters long were used for all computations.

Values of U and V are obtained by differentiating cubic splines fitted to the solutions for the stream function at each grid point and to the boundary values. Pressure coefficients based on the streamwise velocity at the most downstream point on the axis are calculated from the Bernouilli equation so that the variation of the C_p along the contraction walls may be examined. Contours of C_p are also calculated. Further details of the techniques can be found in Watmuff (1985).

EXPERIMENTAL VERIFICATION

To test the approximation of axial symmetry made for octagonal sections and the assumption of inviscid flow, the C_p distribution for the existing LSWT contraction shape was calculated for comparison with experimental measurements. The equivalent radius of the axisymmetric contraction was determined from the octagonal cross-sectional area at 12 axial positions. The dimensions of the octagonal sections were taken from a drawing which was used to construct a 1/3.44 scale model of the LSWT known as the Pilot tunnel. The calculated wall

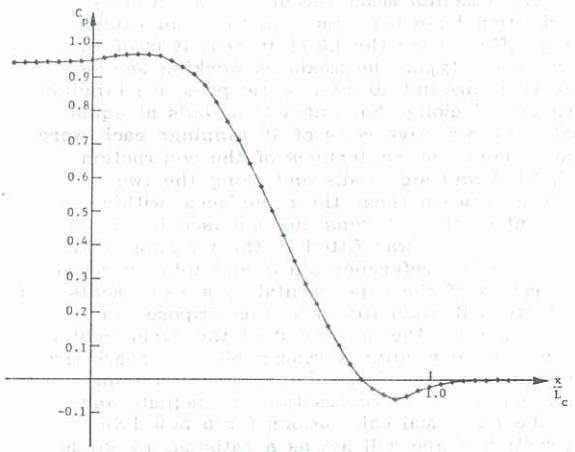

Figure 1. Calculated wall C_p distribution for the Low Speed Wind Tunnel (LSWT) at Aeronautical Research Laboratories (ARL).

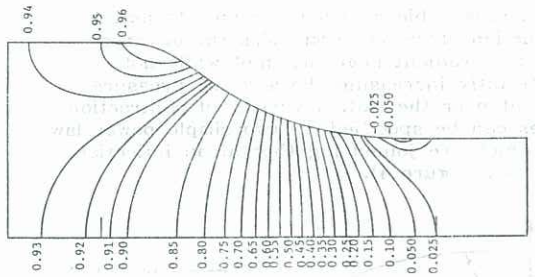

Figure 2. Calculated contours of C_p within the LSWT contraction.

pressure coefficients, shown in Figure 1, are characterized by an almost constant value of C_p from the beginning of the parallel-walled entry section (C_p = 0.9375) to near the entry of the contraction where an abrupt change to a region of almost constant pressure gradient occurs for about 1/8 of the contraction length. The pressure coefficient levels off to a maximum value of 0.966 before falling to a minimum value of -0.062 near the contraction exit. A short region of adverse pressure gradient follows the C_p minimum which is about twice the magnitude of the adverse pressure gradient near the inlet. The contours shown in Figure 2, indicate that the influence of the contraction extends further upstream than downstream. At the end of the contraction the entry flow to the working section is uniform to within around ± 1%.

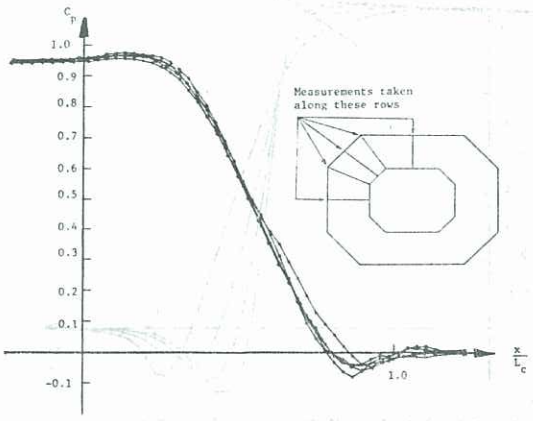

Figure 3. Calculated and experimental values of C_p for LSWT contraction shape.

Experimental measurements of the wall C_p distribution have been made in the Pilot tunnel which differs from the LSWT in that it is of the open return type. The maximum working section velocity is around 20 m/s. Static pressure tappings were placed along the contraction walls at equal axial intervals. Five rows of 46 tappings each were located along the centerlines of the contraction roof, fillet and side walls and along the two vertices between these three surfaces, within one quadrant of the octagonal section (see Figure 3). A Pitot-static tube was fitted in the working section to provide the reference static and total pressure. The results of the experimental C_p measurements and the numerical calculation are superimposed in Figure 3. Since the agreement of the experimental and numerical results is reasonable it appears that the approximation of circular symmetry for an octagonal-sectioned contraction is adequate and that the numerical calculations for a new LSWT contraction shape will act as a satisfactory guide for predicting its performance.

SELECTION OF A NEW CONTRACTION SHAPE

A reasonable criterion for an alternative contraction shape is to minimize the adverse pressure gradient near the inlet while not significantly increasing the adverse pressure gradient near the exit. A variety of contraction shapes can be specified by two simple power law arcs which are joined together at an inflection point (see Figure 4).

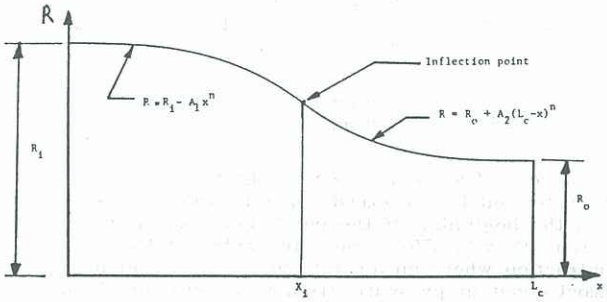

Figure 4. Notation for contraction wall contour. A_1 and A_2 are matching constants and exponent n controls the steepness of the contraction shape.

From intuition, one would expect that the position and magnitude of the adverse pressure gradients near the inlet and outlet of a contraction to be simply related to the wall curvature distribution. Morel tested six contraction curves of order n = 2, 2.5, 3.0, 3.5, and 4.0 all of which had the same contraction ratio (9:1), length to inlet diameter ratio (L_c/D_i = 1) and nondimensional distance from the inlet to the inflection point ($X = X_i/L_c$ = 0.5). As the exponent is reduced, the wall curvature near the entry and exit decreases so that the pressure extrema and adverse pressure gradients also may be expected to decrease. However, Morel's computations indicate that this only occurs for exponents greater than 3.

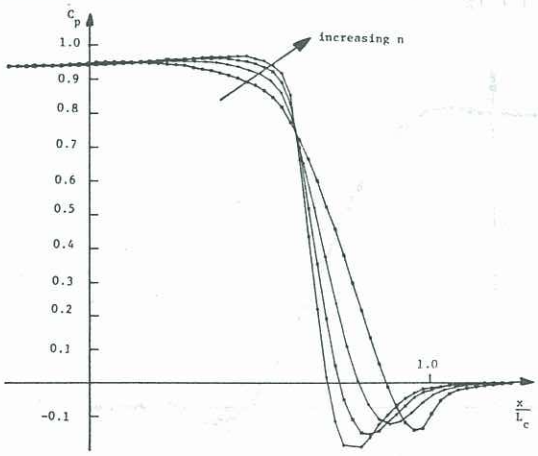

Figure 5. Calculated wall C_p variations for contractions given by L_c/D_i = 0.881 (same as LSWT). X_i/L_c = 0.6 and n = 2, 3, 4 and 5 Arrow shows order of increasing n.

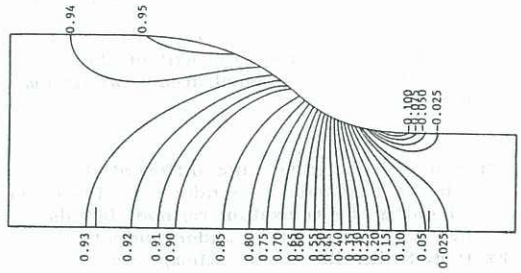

Figure 6. Contours of C_p within contraction specified in Figure 5 with n = 3.

To check that this rather surprising result also occurs for the 4:1 contraction ratio of the LSWT, the C_p distributions for the contraction curves given by n = 2, 3, 4 and 5 were calculated. All the contraction curves had the same nondimensional distance to the inflection point (X = 0.6) and length-to-inlet-diameter ratio of the LSWT (L_c/D_i = 0.881). The wall C_p distributions shown in Figure 5 indicate that as n varies from 3 to 5, the entry and exit C_p extrema and adverse pressure gradients increase. Although the C_p maximum is small for n = 2, the adverse pressure gradient is still relatively large. For n = 2 the C_p minimum near the exit is larger than for n = 3 and the adverse pressure gradient is larger than all the other contraction curves. The ratios of the adverse pressure gradients to those estimated from the LSWT contraction calculation are approximately 0.40, 0.25, 0.36 and 0.67 near the entry and 4.3, 2.3, 2.6 and 3.3 near the exit for the contraction shapes given by n =2, 3, 4 and 5 respectively. The C_p contours for n = 3 shown in Figure 6 indicate that the greatest proportion of the working section length is required on the axis for the velocities to rise to within about 1% of the downstream reference velocity i.e. less working section length is required for the velocity overshoot at the boundary to fall to within the same tolerance.

Compared to the existing LSWT contraction, the third order contraction shape has an inlet adverse pressure gradient which is smaller by a factor of 4

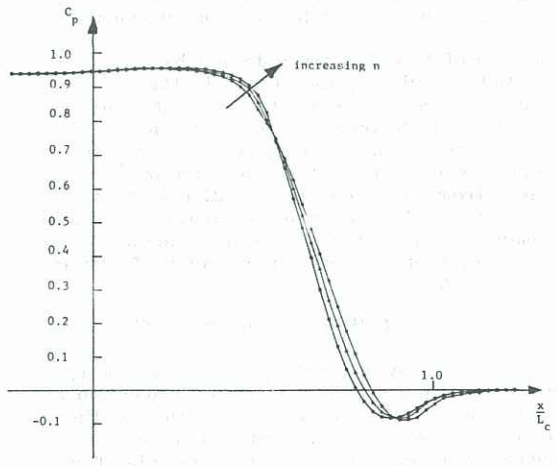

Figure 7. Calculated wall C_p distribution for X_i/L_c = 0.5, L_c/D_i = 0.881 and n = 2.5, 2.75 and 3. Arrow shows order of increasing n.

while the adverse pressure gradient near the exit is larger by a factor of 2.3 If the exponent n is held constant, the effect of moving the inflection point towards the contraction entry would be to decrease the curvature near the exit and increase the curvature near the entry. Hence, the C_p minimum and the adverse pressure gradient near the exit would decrease at the expense of increasing the C_p maximum and adverse pressure gradient near the entry. Therefore solutions were obtained for the cubic contraction shape with X = 0.5 and L_c/D_i = 0.881. Calculations were also performed for contraction shapes with n = 2.5 and n = 2.75 to further examine the curious affect noted earlier regarding the C_p distributions for n < 3. The wall C_p distributions are shown in Figure 7. The adverse

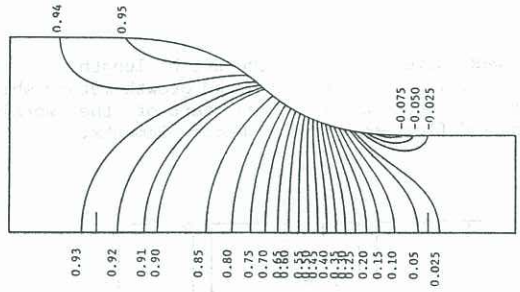

Figure 8. Contours of C_p within contraction specified in Figure 7 with n = 3.

pressure gradients near the contraction entry are all of similar magnitude. However, the contraction shape given by n = 3 offers the smallest C_p undershoot and adverse pressure gradient near the exit. The contours for the case n = 3 are shown in Figure 8 and indicate that the entry flow to the working section approaches uniformity more rapidly than the case where n = 3 and X = 0.6 (see Figure 6). As may be expected from the wall curvature distribution, the upstream influence of the contraction is greater for the case X = 0.5 than for X = 0.6. The entry/exit pressure gradients are approximately 0.38 and 1.65 times those calculated for the LSWT contraction.

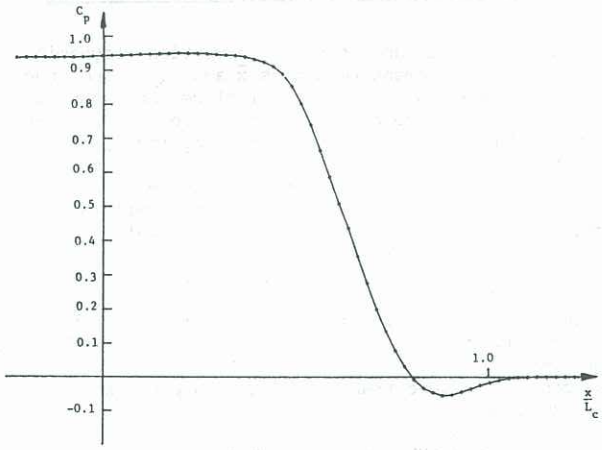

Figure 9. Calculated wall C_p distribution for contraction with X_i/L_c = 0.5, L_c/D_i = 1 and n = 3.

It appears that to achieve the criterion stated earlier for a new LSWT contraction it is necessary to increase the contraction length. Modern contractions usually have a length to inlet diameter ratio around 1 (Mikhail 1979). The calculated wall C_p distribution for the contraction shape specified by n = 3, X = 0.5 and L_c/D_i = 1 is shown in Figure 9. The inlet and outlet pressure gradients are approximately 0.20 and 0.91 times those calculated for the LSWT contraction. This contraction satisfies the criterion of reducing the entry adverse pressure gradient (by a factor of 5) while not increasing the adverse pressure gradient near the exit. The pressure coefficient contours shown in Figure 10 indicate that the upstream and downstream influence of this contraction shape is small. In particular the flow at the exit of the contraction is uniform to within around ± 1%.

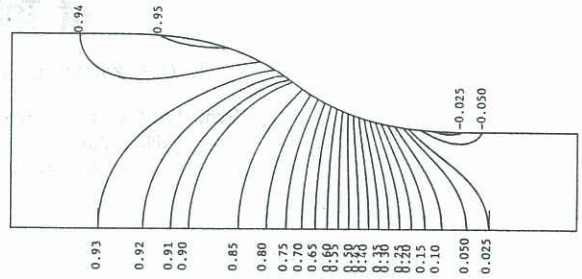

Figure 10. Contours of C_p within contraction specified in Figure 9.

Acknowledgements

The experimental work was performed while the author was employed at the Aeronautical Research Laboratories (ARL), Melbourne Australia. The preparation of this paper was supported by AFOSR Grant No. 85-0126, monitored by Dr. James McMichael and AFOSR Contract No. F49620-84-C-0086 monitored by Dr. James Wilson.

REFERENCES

Barger, R.L. and Bowen, J. T., 1972., "A generalized theory for the design for contraction cones and other low-speed ducts," NASA TN D6962.

Batchelor, G. K. and Shaw,F. S., 1944., "A consideration in the design of wind tunnel contractions," Australian Conference for Aeronautics Report ACA-4.

Bradshaw, P., 1973,. "Effects of streamline curvature on turbulent flow," AGARDograph 169.

Cohen, M. J. and Ritchie, N. J. B., 1962., "Low speed three-dimensional contraction design," J. Roy. Aero. Soc., Vol. 66., pp. 231.

Mikhail, M. N., 1979., "Optimum design of wind tunnel contractions," AIAA Journal, Vol. 17, pp. 471.

Morel, T., 1975., "Comprehensive design of axisymmetric wind tunnel contractions," Trans. ASME, J.Fluids Eng., pp. 225.

Smith, G. D., 1978., "Numerical solutions of partial differential equations: finite difference methods." Second edition, Clarendon Press, Oxford.

Smith, R. H. and Wang, C. T., 1944., "Contracting cones giving uniform throat speeds," J. Aeronautical Sci. Vol. 11, pp. 356.

Szczenioski, B., 1943., "Contraction cone for a wind tunnel," J.Roy.Aeronautical Sci., Vol. 10, pp. 311.

Thwaites, B., 1946., "On the design of contractions for wind tunnels," Aero. Res. Council R & M 2278.

Tsien, H., 1943., "On the design of the contraction cone for a wind tunnel," J.Roy. Aeronautical Sci., Vol. 10, pp. 68.

Watmuff, J. H. 1985., "Design of a new contraction for the ARL Low Speed Wind Tunnel." (submitted ARL report)